

N71-20299
NASA CR-117320

THE EFFECT OF ACOUSTIC FIELDS
ON THE
EFFICIENCY OF SOLAR CELLS

NASA GRANT NO. NGR 44-007-006

by

**CASE FILE
COPY**

M. W. Wilcox

and

L. R. Latch

March 8, 1971

TABLE OF CONTENTS

	<u>PAGE</u>
SUMMARY	ii
INTRODUCTION	1
THE p-n JUNCTION	1
THE RESPONSE OF A (p-n) JUNCTION TO A PHOTON INPUT	3
THE MECHANICS OF A (p-n) JUNCTION	4
THE ACOUSTOELECTRIC EFFECT	7
METHODS OF OBTAINING THE ACOUSTOELECTRIC EFFECT	9
DEFORMATION POTENTIAL METHOD	9
COMPARISON OF PIEZOELECTRIC AND DEFORMATION POTENTIAL COUPLING	11
THEORETICAL COMPUTATIONS	15
ACOUSTIC WAVES AND SOLAR CELLS	16
PHONON-PHOTON-ELECTRON INTERACTION IN A PHOTOVOLTAIC SEMICONDUCTOR	16
TEST EQUIPMENT	22
LABORATORY PROCEDURE	25
TEST PROCEDURE	27
LABORATORY TEST RESULTS AND SUMMARY	28
RESULTS AND CONCLUSIONS	29
APPENDIX	31
REFERENCES	32

SUMMARY

Tests were conducted on Gallium Arsenide samples which varied in resistivity due to doping. The most resistive sample (in the range of 50 megohms) showed no response due to sound input. The most efficient cell tested showed approximately 100mv output under normal light intensity. The response to sound was relatively high but was not dependent on the samples' exposure to light.

Silicon solar cells were found to be totally unresponsive to sound input, with or without light exposure.

Several photoresistive devices were tested but there was no indication of direct interaction of light, sound and electron motion.

THE EFFECT OF AN ACOUSTIC WAVE ON THE PHOTO-VOLTAIC PROCESS

BY

M. W. Wilcox and L. R. Latch

INTRODUCTION

This research is pointed toward the use of acoustic fields to enhance the efficiency of solar cells. Through the understanding of the photovoltaic and the acoustoelectric effects one is in a better position to attack the problem of the application of acoustic waves to bodies which are, simultaneously, subjected to the photovoltaic and acoustoelectric effects. The concern in this investigation is therefore with the phonon-photon-electron interaction, and the effect of this interaction on solar cell operation.

The photo-conversion device that has attained the highest efficiency in practice, is the silicon (p-n) junction. (1)(2)*. This type junction is now described because it is this type which is used in the present study.

THE P-N JUNCTION

Consider the diagram shown below which is a schematic for a (p-n) junction.

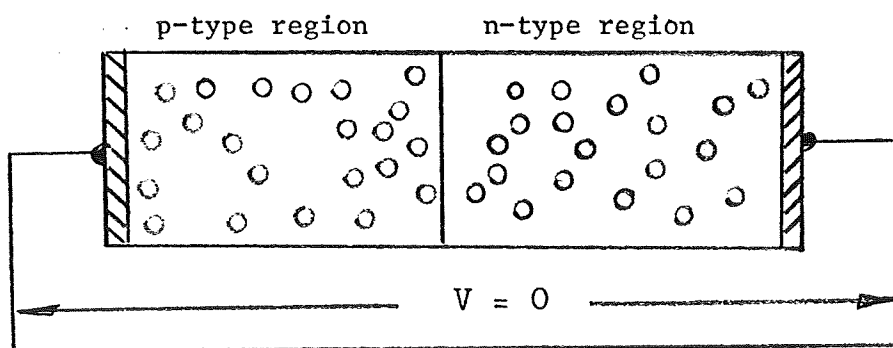


Fig. 1. (p-n) Schematic

One portion of the material is made P-type by the incorporation of suitable acceptors imperfections, and another portion of the same material is made n-type.

*The superscripts refer to the references, appearing at the end of this report.

By the incorporation of suitable donor imperfections, a barrier, called a p-n junction, exists at the point of transition from the p-type portion to the n-type portion. How this barrier arises can be visualized by considering the p-type portion and the n-type portion as originally separated in space, and then brought together. When contact between the two portions are made, electrons flow from the n-type portion into the p-type portion, and holes from the p-type portion into the n-type portion because of the concentration gradients existing. The flow continues, thereby building up a positive charge on the n-type side of the junction and negative charge on the p-type side of the junction, until the diffusion flow caused by the concentration gradients is counterbalanced by the flow in the reverse direction caused by the electric field set up at the junction. A contact potential difference, having an energy $\Delta\xi$ develops across the junction of such a magnitude as to just oppose the further flow of electrons and holes due to the concentration gradient.⁽³⁾ The region adjacent to the junction is said to contain a space charge and is sometimes referred to as a transition region. The extent of this region around the junction is 10^{-4} to 10^{-6} cm wide.

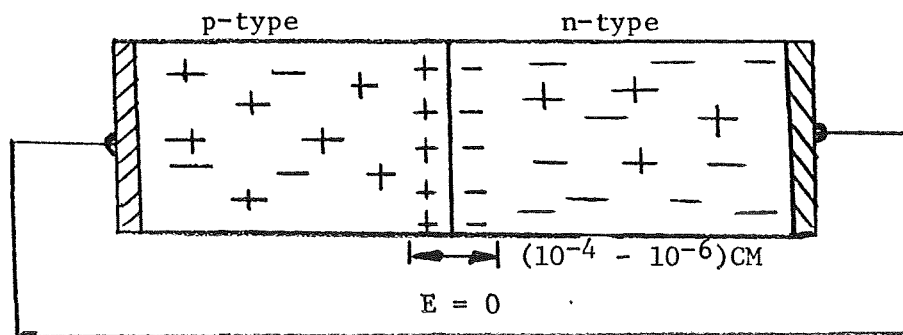


Fig. 2. Equilibrium Condition about the Transition Region

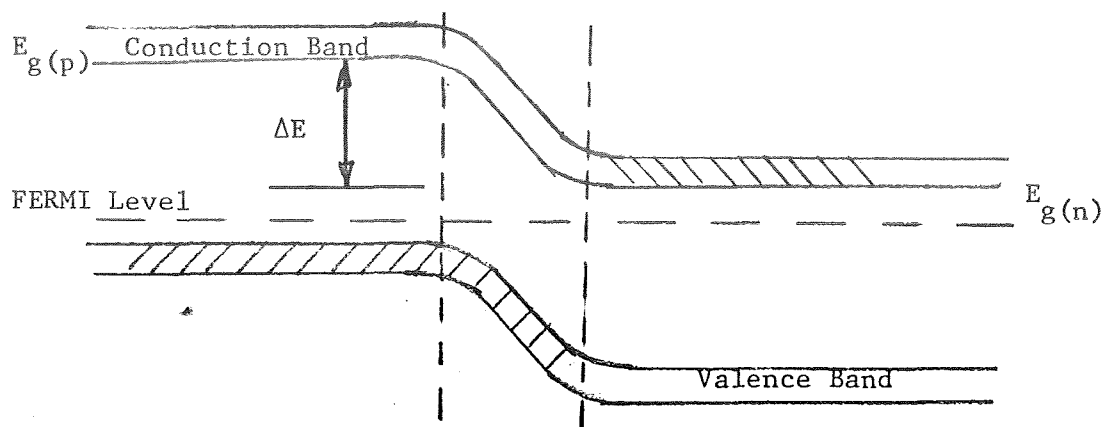


Fig. 3. p-n Junction Schematic Showing the Energy Band Scheme

The energy-level diagram corresponding to the equilibrium condition of Fig. 2 is shown in Fig. 3.

It should be noted that the contact potential across the junction cannot be used to deliver load. This condition is analogous to two containers filled with liquid connected by a pipe in which the liquid seeks the same level in both containers as long as nothing disturbs the system; this is stated formally as: "In a System in thermal equilibrium the FERMI-level energy is constant throughout the entire system". Figs. 2 and 3 depict, schematically, the statements immediately above.

THE RESPONSE OF A (p-n) JUNCTION TO PHOTON INPUT

As stated previously, this research is concerned with the effect of acoustic waves on the efficiency of solar cells. Prior to the investigation of this effect, however, it is well to review the photo-voltaic concept.

The photo-voltaic effect is not a new discovery, of course. Edmund Becquerel noted, as early as 1839, that a voltage was developed when light was directed onto one of the electrodes in an electrolyte solution. This effect was first noted, with respect to solid matter, somewhat later 1877 by W. G. Adams and R. E. Day who carried out experimental work on Selenium. Other early researchers such as

Schottky, Lange and Grondahl, did pioneering work in producing photovoltaic cells with Selenium and cuperous oxide. It was to be more than three quarters of a century after the photovoltaic effect was first noted on solids that researchers turned to the problem of utilizing this effect as a source of power. In 1954 several groups including researchers at the RCA and Bell Laboratories achieved conversion efficiencies of about 6% by means of (p-n) junction. Cadmium sulfide and silicon junctions (p-n) junctions were the materials used in these early devices. Later workers have achieved efficiencies near 15% by using improved silicon junctions.

The photovoltaic action converts electromagnetic radiation directly to electrical power. By eliminating the intermediate step of conversion to heat, we bypass the carnot limitation on efficiency of heat engines.

The production of electrical power by electromagnetic radiation can be carried out by exposing a (p-n) junction to electromagnetic radiation of various types. We are concerned, in this research, with exposing the device to sunlight, whose wavelength is in the range of $5,000 \text{ \AA}$. Hence, the (p-n) junction is, in this case, classified as a photovoltaic converter.

THE MECHANICS OF A (p-n) JUNCTION

Consider again the mechanism by which a (p-n) junction converts light to electrical power delivered to an external load. When the junction region is illuminated with light of sufficiently energetic photons to excite an electron from the valence band state to the conduction band state, the resulting free electron and hole move in response to the built-in electric field that the junction possesses. We may visualize this process as follows:

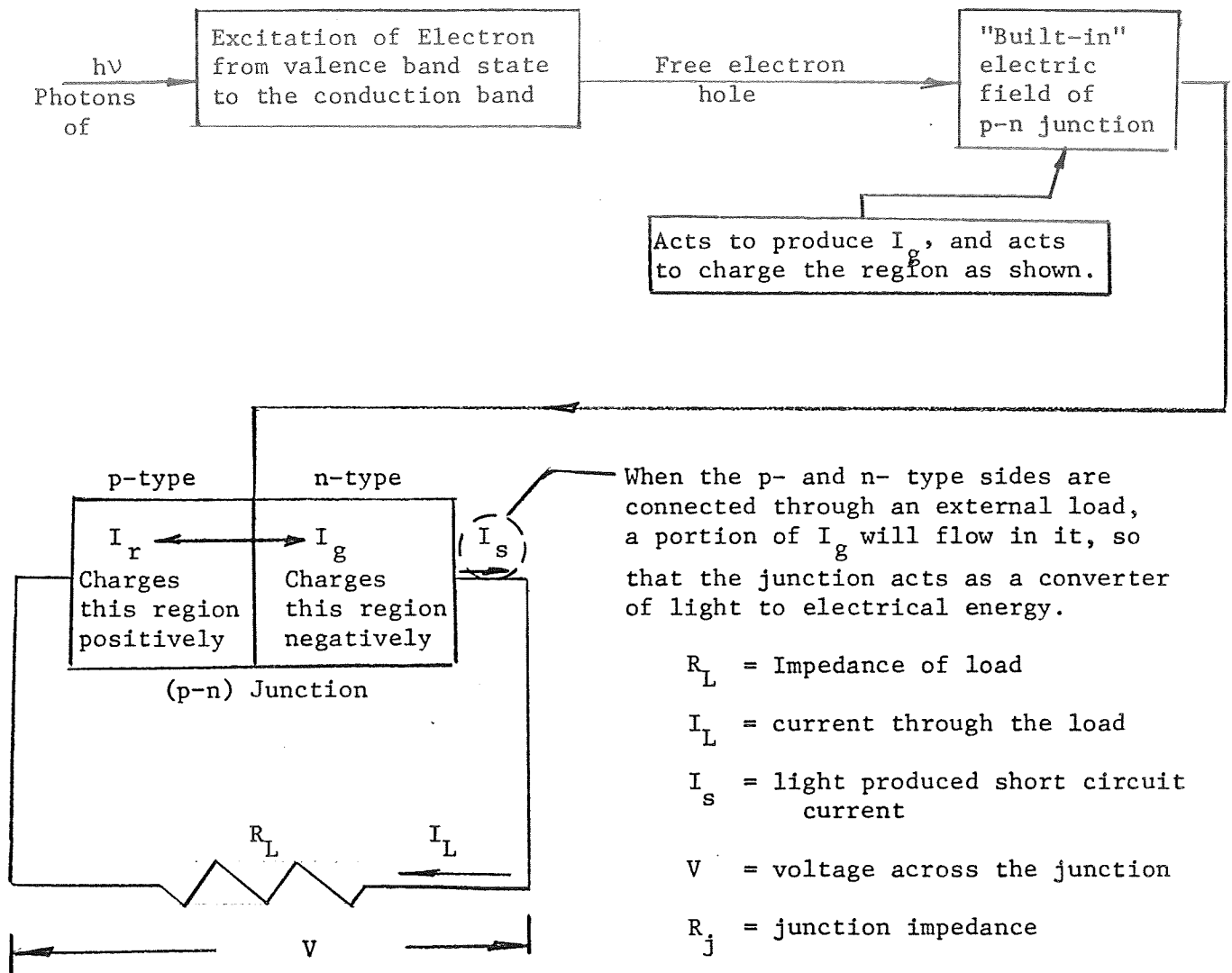


Fig. 4. Mechanics of a (p-n) junction.

The equivalent circuit for the system shown above is as follows: (4)

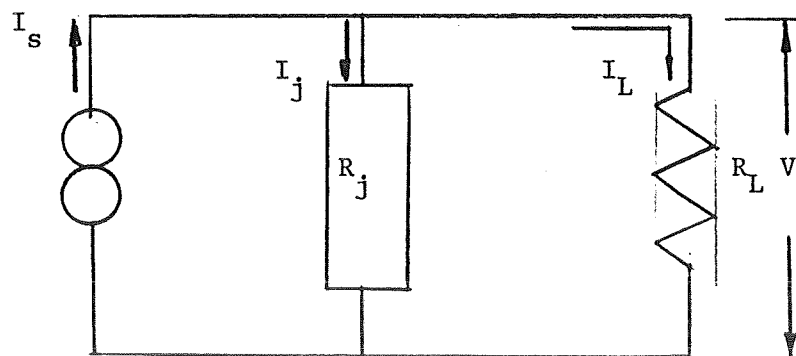


Fig. 5. Simplified Equivalent Circuit for an Illuminated p-n Junction photovoltaic cell

It is to be noted that I_s is the photocurrent that is produced by illumination of a semiconductor which is an insulator in the dark. This current may be expressed as a function of the following variables:

- (a) F' , the total number of electrons and holes produced each second by the absorbed photons
- (b) the effective lifetime, τ^*
- (c) the transit time, T_r

The value of I_s is expressed as

$$I_s = eF'\tau^*/T_r$$

in which e is the electronic charge in coulombs.

The transit time, T_r , is the time spent by an electron in moving between two electrodes connected to the semiconductor. It may be determined from the electrode spacing and the mean drift velocity of the electron to be

$$T_r = \frac{L}{u} = \frac{L}{\mu E}$$

in which

u = means drift velocity

μ = drift mobility

E = Applied electric field

now $E = \frac{V}{L}$ in which V = Applied voltage and L = interelectrode spacing. We thus have,

$$T_r = \frac{L^2}{\mu V}$$

The larger the effective lifetime τ^* the greater will be the photocurrent I_s . If we imagine that the lifetime of an electron is greater than the lifetime of a hole, this means that holes are trapped quickly in recombination centers+ while the free electron exists long enough to be swept out of the crystal by the applied field. Since charge neutrality must be preserved, the negative electrode ejects another electron until the free electron can recombine to be made available for conduction. This apparent gain is denoted by a gain factor which is a direct index to the efficiency of a photoconductor, as can be seen from its effect on I_s .

+See Ref. 1, footnote, p. 99

$$G = \frac{\tau^*}{T_r}$$

It can be seen that the discussion of I_s in the sense just described is on a microscopic scale whereas the description of the mechanics of a (p-n) junction as described in Figs. 4 and 5 is on a macroscopic basis. The current I_s , shown in Fig. 4, is to be considered now in the macroscopic sense and can be thought of as being produced by a constant current generator, delivering the current I_s into network of impedances. A simplified equivalent circuit in the macroscopic sense is shown in Fig. 5.

THE ACOUSTOELECTRIC EFFECT

When a sound wave propagates through a material containing conducting electrons, its momentum, as well as its energy, is attenuated by the electrons.⁽⁵⁾ The momentum attenuation acts as a dc force causing the electrons to drift in the direction of the force. If there is a closed circuit in this direction, a direct current will be produced. This is the acoustoelectric current; it is proportional to the sound intensity, since the momentum itself is proportional to the sound intensity. If, on the other hand, the circuit is open, the drifting electrons produce a space charge whose electric field cancels the dc force due to the sound wave momentum attenuation. This back EMF is the acoustoelectric field.

The acoustoelectric effect was first predicted by Parmenter.⁽⁶⁾ His explanation concerning the physical characteristics associated with this effect were qualitative in nature but quite logical in content. On the basis of Parmenter's reasoning, we consider the effect on conduction electrons of a crystal resulting from a single travelling longitudinal acoustic wave in a crystal. Consider this travelling acoustic wave to be sinusoidal in nature (which will be the case for small amplitude acoustic waves). This wave gives rise to a sinusoidal electric

field which travels through the crystal with the same velocity as that of the acoustic wave. Consider now conduction electrons which are contained in the crystal, and undergoing certain motions. Some of these electrons will be travelling such that they will have components of velocity that are parallel to the acoustic wave travel. For most of these conduction electrons, this component of velocity will be much larger than the acoustic wave speed so that these electrons are "out of phase" with respect to the travelling electric field. Thus, the time average of this field over their trajectories is zero and these electrons are essentially unaffected by the presence of the acoustic wave. There are a few electrons, however, having components of velocity parallel to the acoustic wave which are comparable to the speed of the wave. These electrons are capable of being trapped by the moving electric field so that this time-averaged velocity in the direction of the field is exactly that of the field. Among these electrons, those having a maximum energy will be found to give rise to a net electric current. In a metal, these electrons are at the Fermi-level. In an n-type semiconductor, these electrons are in the conduction band. Such a generation of an electric current by a travelling acoustic wave may be called the acoustoelectric effect. As pointed out by Parmenter, it is interesting that the qualitative explanation of this effect which has just been given is analogous to the qualitative explanation of the operation of a linear accelerator.⁽⁷⁾ A further physical interpretation of the acoustoelectric effect may be obtained by viewing the sketch shown below:

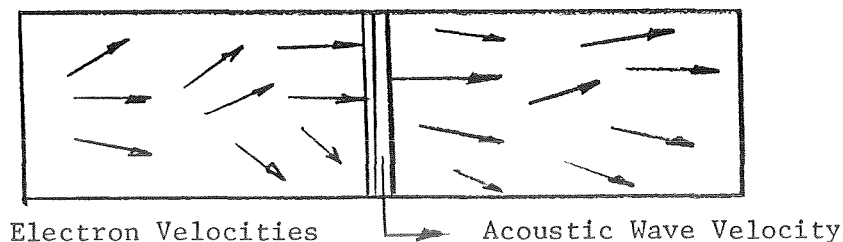


Fig. 6. some components of electron velocities are equal to the wave velocity. These components amplify the acoustic effects.

METHODS OF OBTAINING THE ACOUSTOELECTRIC EFFECT

There are two means of obtaining the effect described above. These are (1) the perturbation potential or deformation potential method and (2) the piezoelectric method. Both of these means are described qualitatively by the section on THE ACOUSTOELECTRIC EFFECT immediately preceeding this section. Each of these specific ideas will now be examined in more detail and discussed relative to their analytical and experimental treatment.

DEFORMATION POTENTIAL METHOD*

For a cubic crystal such as silicon, diamond, or germanium, subject to a homogeneous strain, ϵ_{ij} (say), the linear shift in energy band with strain may be expressed in the form⁽⁸⁾

$$E = E_o + \sum \beta_{ij} \epsilon_{ij} = E_o + E_1 \Delta$$

where,

$\Delta = \epsilon_{11} + \epsilon_{22} + \epsilon_{33}$ is the dilatation. The term E_o is the correct potential in the absence of the acoustic wave and $E_1 \Delta$ results from the changes in interatomic spacing set up by the acoustic wave. Shifts in the energy levels corresponding to the top of the filled band, E_f , and the bottom of the conduction band, E_c , produced by a periodic dilatation of a lattice wave are shown schematically below. As illustrated, the bands may shift in opposite directions. In a crystal with the diamond structure (such as silicon, for instance) the energy gap, E_g , decreases with positive dilatation; in others such as Te, the shift is in the opposite direction.

*A detailed comparison of deformation-potential and piezoelectric coupling is given by Mertsching⁽⁹⁾.

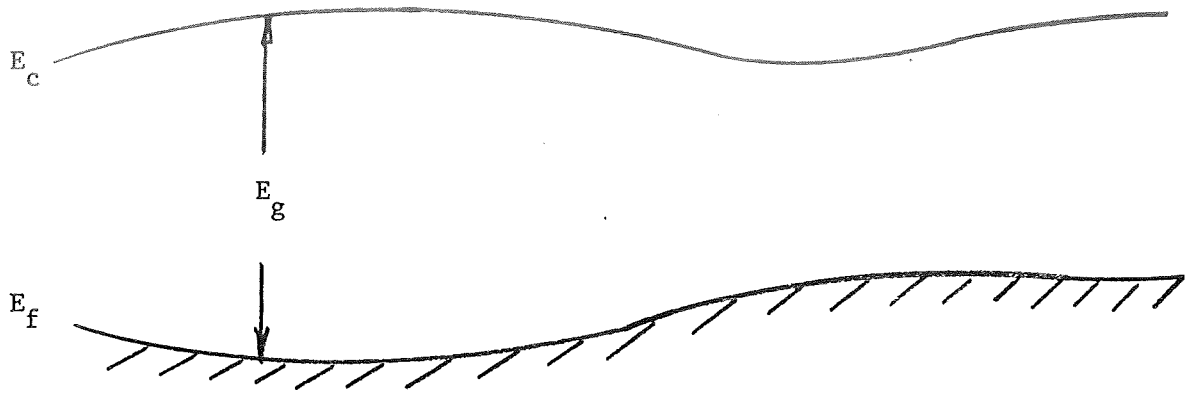


Fig. 7. Shift of Energy Bands with Varying Dilatation

Parmenter ⁽⁶⁾ makes use of the idea discussed above. Starting with the potential acting on an electron in the unstrained crystal, he expresses the effect of the dilatation on a given portion of the band by adding to the original potential a constant perturbative potential equal to the shift in energy of that portion of the band. This perturbative potential is called the deformation potential. This basic idea is due to Shockley and Bardeen.⁽⁸⁾ The assumption is then made that such a procedure is also valid for non-uniform dilatations of the crystal, whereupon a non-uniform deformation potential is required. This assumption seems plausible provided that the dilatation varies very slowly with position (on the atomic scale) i.e. the dilatation results from a long wavelength acoustic wave. The deformation potential is taken to be proportional to the dilatation. Thus, if the acoustic wave is represented by

$$\bar{s} = \bar{S} \sin \bar{\sigma}(\bar{r} - \bar{c}t).$$

Then the deformation potential is given by

$$V_{lb} = A' \bar{\nabla} \cdot \bar{S}$$

in which

\bar{s} = displacement vector

\bar{S} = amplitude vector

$\bar{\sigma}$ = acoustic wave vector

\bar{c} = wave velocity

A' = an assumed constant of proportionality

According to Parmenter, the one electron approximation using Schrödinger's equation by making use of the deformation potential mentioned previously, may then be solved.

COMPARISON OF PIEZOELECTRIC AND DEFORMATION POTENTIAL COUPLING⁽¹⁰⁾

The basic property of a piezoelectric crystal is that a mechanical strain produces an electric field which is proportional to the strain. In a non-piezoelectric crystal, a deformation of the lattice structure produces a change in the potential energy of a conduction electron which is proportional to the strain. This latter perturbation caused by a deformation of the lattice structure is known as the deformation potential. It can be written as ⁽¹¹⁾

$$U_d = C_d S$$

in which, evidently S represents plan strain and C_d is a deformation coupling constant.

The magnitude of the electric field produced in a piezoelectric insulator by a strain S is given by

$$E = \frac{e}{\xi} S$$

If S is the result of an acoustic wave, this field corresponds to a change in the potential energy of an electron which is given by

$$U_p = \frac{qe}{\xi k_s} \equiv C_p S$$

in which, evidently

e = piezoelectric constant

q = electronic charge

ξ = dielectric constant

$k_s = 2\pi/\lambda$

λ = acoustic wavelength

The constant C_p is referred to as the electron-phonon coupling constant.

According to J. H. McFee⁽¹⁰⁾, a measure of relative strength of the effects on

the transmission and amplification of acoustic waves due to the deformation potential coupling and those due to piezoelectric coupling is given by the ratio

$$\frac{C_d^2}{C_p} = \left(\frac{\xi C_d}{q v_s} \right)^2 \omega^2$$

The significance of leaving the terms squared in the above ratio is that the acoustic attenuation is proportional to the square of the coupling constant.

McFee⁽¹⁰⁾ compared the piezoelectric semi-conductor cds with the non-piezoelectric semi-conductor Germanium on the basis of the ratio above. The following values were assigned to the quantities of the equation

$$\begin{aligned} \left(\frac{C_d}{C_p} \right)^2 &= \left(\frac{\xi C_d}{q v_s} \right)^2 \omega^2 ; \\ C_d(\text{Ge}) &= 10\text{ev} = 1.6 \times 10^{-18} \text{ joule} \\ e(\text{CdS}) &= 0.2 \text{ coulomb/meter} \\ \xi &= 9\xi_0 = 8 \times 10^{-11} \text{ Farad/meter} \\ v_s &= 4 \times 10^3 \text{ meter/sec.} \\ q &= 1.6 \times 10^{-19} \text{ coulomb} \end{aligned}$$

Hence, there is obtained

$$\left(\frac{C_d}{C_p} \right)^2 \approx 10^{-24} \omega^2$$

At the ultrasonic frequency of 50 MC $(C_d/C_p)^2 \approx 10^{-7}$. Hence, deformation potential effects in Germanium are very small compared with the corresponding piezoelectric effects in cadmium sulfide at Ultrasonic frequencies. The two types of effects are about equal at an acoustic frequency of 100 KMc and the deformation potential dominates at still higher frequencies. Microscopic theory, $(k_s \ell \gg 1)$, is usually valid only at very high frequencies where the deformation-potential coupling is comparable with the piezoelectric coupling (for example, in Cds, at room temperature, $k_s \ell \approx 1$ at an acoustic frequency of 30 KMc)

In a study by Hutson, McFee and White, ⁽¹²⁾ following a suggestion by White, the attenuation in Cds was studied in the presence of an externally applied drift field. White realized that the same mechanism which causes positive acoustic attenuation in the absence of electron drift should cause negative attenuation (acoustic amplification) when the drift velocity exceeds the acoustic wave velocity. Earlier, from a theoretical analysis of the effects of conduction electrons on acoustic propagation in nonpiezoelectric semiconductors, Weinrich ⁽¹³⁾ (1956) had predicted that the electronic contribution to acoustic attenuation would become negative when the drift velocity exceeded the sound velocity. The experimental arrangement was a simple one and its essentials are shown below.

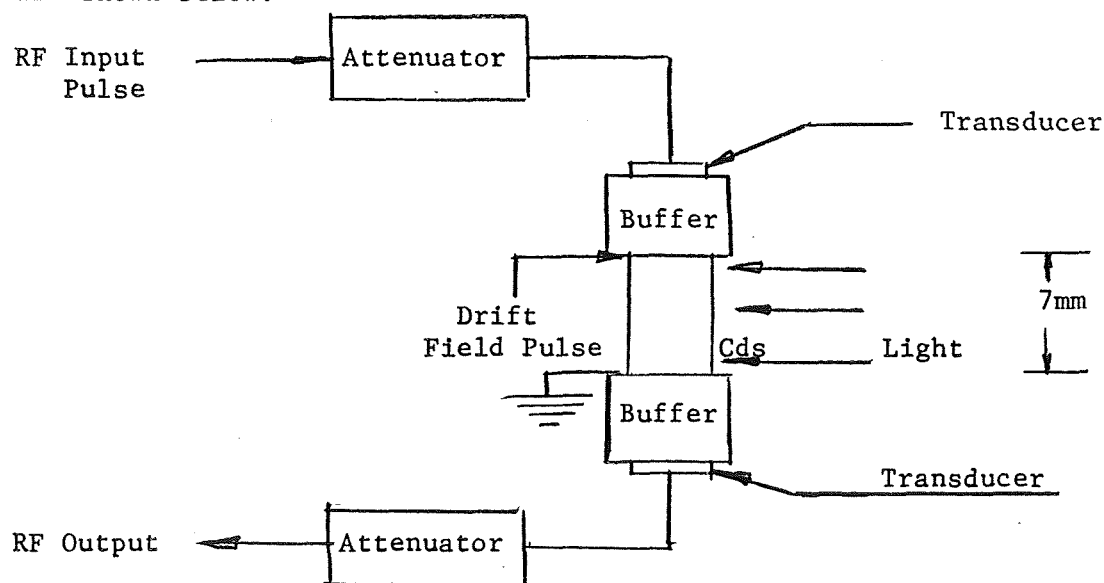


Figure 8. Experimental Arrangement for Amplification Study
After Weinreich ⁽¹⁵⁾

One microsecond pulses of 15 Mc (or 45 Mc) shear waves produced at the upper transducer passed down through the Cds crystal and were detected at the lower transducer. The Cds crystal was oriented so that the shear wave was piezo-electrically active, e.e. the shear wave propagated in a plane perpendicular to the Cds hexagonal axis, with particle motion along the hexagonal axis. Transit time through the 7mm Cds sample was approximately 4 microsecond (4μ sec). Conduction electrons were produced in the sample by illumination with yellow light from a high pressure mercury arc (5770/5790 Å). Under the illumination, the sample resistivity was in the range of 10^4 to 10^5 ohm-cm. When the sample was unilluminated ("dark condition") it was essentially insulating. The shear wave signal level obtained in the "dark" condition served as the zero attenuation reference in these experiments. Diffused indium ohmic contacts were made to the entire top and bottom surface of the Cds. A drift-voltage pulse of approximately 5 microsecond duration could be applied between these contacts during the time of transit of the signal through the Cds. A low drift duty cycle was used to avoid heating the sample.

The observed effects of the electron drift on the ultrasonic attenuation are shown in Fig. 9 below.⁽¹²⁾ Postive values of drift field mean that the electrons are drifting in the direction of sound propagation. The data of Fig. 9 above correspond to a relatively high level of illumination (sample resistivity 3×10^4 ohm cm). First it should be noted that for drift fields greater than 700 v/cm the ultrasonic attenuation becomes negative, i.e. the output signal is larger than the signal obtained under dark conditions. Furthermore, if an electron mobility of $300 \text{ (cm}^2/\text{volt sec)}$ is taken from Hall measurements made on Cds crystals at room temperature), the crossover from positive to negative attenuation is found to correspond to a drift velocity of about 2×10^5 cm/sec. The shear-wave velocity is 1.75×10^5 cm/sec. Thus, White's prediction of ultrasonic amplification for drift velocities greater than the sound velocity is verified.

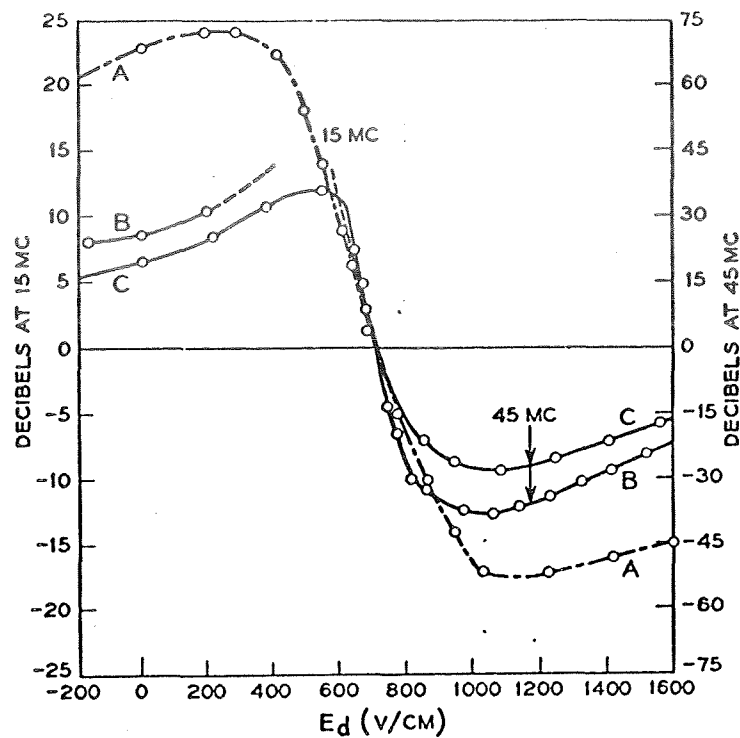


Figure 9. Observed ultrasonic attenuation in 7mm CdS sample as a function of drift field. Zero decibels represent attenuation with sample illuminated. Curve A: $\omega_c/\omega = 0.24$. Curve C: $\omega_c/\omega = 0.21$. After Hutson, et al (1961)

THEORETICAL COMPUTATIONS

It is to be noted in the work by Hutson discussed above, that at ultrasonic frequencies in Cds, $k_s \ell \ll 1$ so that macroscopic theory applied.

The interaction of acoustic waves with mobile carriers is most conveniently discussed in two limiting regimes, $k_s \ell \ll 1$ and $k_s \gg 1$ ($k_s = 2\pi/\lambda$, where λ is the acoustic wavelength, and ℓ is the mean free path of the carriers) at ultrasonic frequencies. λ is usually large compared with ℓ so that $k_s \ell$ is considerably less than unity. This theory is macroscopic in the sense that the acoustic wave is treated as a classical wave which perturbs the carrier distribution. The theory then describes, in a self-consistent way, how the carrier distribution adjusts itself to the presence of the acoustic wave. Furthermore, the electrical conductivity is used to simply relate the current caused by the acoustic wave to the self-consistent electric field. The fact that the carriers are scattered many times per λ makes possible the simplifying assumptions of macroscopic theory.

The other limiting regime $k_s \ell \gg 1$ is associated with studies at much

higher frequencies and are usually associated with studies making use of the deformation potential, at frequencies of 100 KMc (10" Hertz). This frequency regime is at a level in which deformation potential effects become important as opposed with piezoelectric effects which are important in the 15Mc to 45 Mc range.

ACOUSTIC WAVES AND SOLAR CELLS

We may now more easily show the present effort of studying the effect of acoustic waves on solar cells by drawing a comparison of what has taken place in ultrasonic amplification, which has been discussed previously and the idea which is investigated in this endeavor.

We remember in our discussion of ultrasonic amplification that it was shown by Hutson et al (12) that an Rf pulse input into a sample of piezoelectric material of Cds under the condition shown in Fig. 8, resulted in sound (acoustic) amplification on the output side of the sample. Hence, it was seen that there exists a coupling interactive result between phonon injection and electron motion to result in either sound amplification (negative attenuation) or sound suppression (positive attenuation).

The final effects that concerned the present investigators were those of the interaction of photons, phonons and electrons and to thereby establish the possiblility of the change of the efficiency of solar cells by this 3-non interaction*

PHONON-PHOTON-ELECTRON INTERACTION IN A PHOTOVOLTAIC SEMICONDUCTOR

The "3-non" coupling can be likened to the operation of a simple triode where the phonon acts as the controlling element. The purported action of the phonon is to create a non-equilibrium electronic state which is receptive to the impinging photon spectrum to higher than otherwise degree. The inverse action is not considered although surely the electron must play an intermediate role in photon generation of phonons.

*3-non is used here as an abbreviated term referring to phonon-photon-electron interaction

higher frequencies and are usually associated with studies making use of the deformation potential, at frequencies of 100 KMc (10" Hertz). This frequency regime is at a level in which deformation potential effects become important as opposed with piezoelectric effects which are important in the 15Mc to 45 Mc range.

ACOUSTIC WAVES AND SOLAR CELLS

We may now more easily show the present effort of studying the effect of acoustic waves on solar cells by drawing a comparison of what has taken place in ultrasonic amplification, which has been discussed previously and the idea which is investigated in this endeavor.

We remember in our discussion of ultrasonic amplification that it was shown by Hutson et al (12) that an Rf pulse input into a sample of piezoelectric material of Cds under the condition shown in Fig. 8, resulted in sound (acoustic) amplification on the output side of the sample. Hence, it was seen that there exists a coupling interactive result between phonon injection and electron motion to result in either sound amplification (negative attenuation) or sound suppression (positive attenuation).

The final effects that concerned the present investigators were those of the interaction of photons, phonons and electrons and to thereby establish the possiblility of the change of the efficiency of solar cells by this 3-non interaction*

PHONON-PHOTON-ELECTRON INTERACTION IN A PHOTOVOLTAIC SEMICONDUCTOR

The "3-non" coupling can be likened to the operation of a simple triode where the phonon acts as the controlling element. The purported action of the phonon is to create a non-equilibrium electronic state which is receptive to the impinging photon spectrum to higher than otherwise degree. The inverse action is not considered although surely the electron must play an intermediate role in photon generation of phonons.

*3-non is used here as an abbreviated term referring to phonon-photon-electron interaction

A rather vigorous study of solar cell performance has been made since Chapin, Fuller and Pearson first utilized a p-n junction in silicon as a solar energy converter in 1954⁽¹⁴⁾. Naturally the primary interest has been in increasing the solar cell efficiency by geometry of the configuration, material doping, design of collector grids, addition of antireflectant coatings, and theoretically by utilization of drift fields arising from density gradients of impurities. More recent studies have been directed toward the use of multi-layered and multi-transition cells. The actual performances of both the primitive and the improved cells, however, have never reached their theoretically predictable maximum efficiency. The basic equations describing the characteristics of photovoltaic solar energy converters and the corresponding equivalent circuit are given in references 15-17. Some typical comparisons are given below in Table 1.

Table I - Solar Cell Efficiency⁽⁴⁾

<u>Material</u>	<u>Type</u>	<u>Efficiency Attained</u>	<u>Maximum Predicted</u>
Si	Single Crystal	15%	20%
InP	Alloy on n-base	2	23
GaAs	Zn diffused p on n-base	9	24
CdTe	"	4	21
Cu ₂ O	Polycrystalline	1/2	-
Se	", p-n junction between two different materials	1	-
GaP		<1/2	17
DcS	Single Crystal	6	16
	Evaporated Film	3	

Single layer polar cells utilize only about 46 percent of the sun's energy, whereas the multi-layered cells are predicted to utilize approximately 69 percent based upon gradation of energy gaps.

The limitations on the efficiency of photovoltaic solar energy converters can be broken down into the following major factors according to Wolf⁽¹⁸⁾:

1. Reflection losses on the surface;
2. Incomplete absorption;
3. Utilization of only a part of the photon energy for the creation of electron-hole pairs;
4. Incomplete collection of the electron-hole pairs by diffusion to the p-n junction;
5. A voltage factor given by the ratio of open circuit voltage to energy gap potential difference;
6. A curve factor given by the ratio of maximum power point voltage time maximum power point current to open-circuit current for an ideal p-n junction;
7. Additional degradation of the curve due to internal series resistance.

Items 1, 4, and 7 are determined by fabrication techniques and improvement on these may be possible up to near elimination of their influence Wolf considers items 2,3,5, and 6 as having absolute physical limitations beyond which improvement is not possible. As stated previously (p.1) it is the intent of this study to investigate the possibility of improvement in the absorption and utilization of photons absorbed by phonon injection with resultant coupling with the photon-electron interaction. An improvement of items 2 and 3 should also exhibit an improvement in item 6 but may show a slight reduction in output voltage, which is not considered to be extremely objectionable.

Observations were made in the laboratory of the result of phonon generation in at least two different types of photovoltaic solar generators, the effect being indicated by a deviation of output voltage and output current of the device in concurrence with the traveling sound wave. Variations which are immediately

convenient might include the illumination intensity and the external load impedance; with severe limitations, also the sound frequency and sound intensity. The latter two parameters may be the most important criteria in establishing the dual coupling of the "3-non" interaction.

The photon-electron coupling is demonstrated first by photoconductivity and to a higher degree by the photoelectric effect. Photoconductive materials may be utilized as electromagnetic radiation detectors, whereas photoelectric (or photovoltaic) materials are used as energy converters where solar radiation is transformed to electrical energy. Quantum electronics is the basis of analyzing processes in both types of materials. In discussing photoconductivity of solid materials in crystalline form, Bube⁽¹⁹⁾ states that the presence of phonons affects the occupation of energy levels and the transport of charge through the crystal, but does not by itself introduce any new levels. His statement should be interpreted as "any additional levels," since the number of energy eigenvalues are characteristic of the material. When the crystal lattice structure is subjected to a traveling sound wave, however, both the energy gap and the quantum levels change with the number of quantum states remaining invariant⁽²⁰⁾. This is one phenomena which would tend to induce additional coupling between the photon and the electron. It is anticipated that such an effect would be evidenced by a smoothing of the response spectrum of the test sample to an illumination of distributed wavelength such as that of solar radiation. This would be similar to the effect predicted for multi-layered cells.

It may also be noted at this point that the migration of electrons which are normally in the conduction band would be enhanced in the direction of the acoustic wave according to the acoustoelectric phenomena which have been recently reported. The coupling was first interpreted as phonon-wave drag, where the phonon wave transfers momentum to the electron. As explained by Eckstein⁽⁵⁾, when a sound wave propagates through a material containing conduction electrons, its momentum, as

as well as its energy, is attenuated by the electrons. The momentum attenuation acts as a dc force causing the electrons to drift in the direction of the force. If there is a closed circuit in this direction, a direct current will be produced. This is the acoustoelectric current; it is proportional to the sound intensity, since the momentum attenuation is itself proportional to the sound intensity. If on the otherhand the circuit is open, the drifting electrons produce a space charge whose electric field cancels the dc force due to the sound wave momentum attenuation. This back electric field is the acoustoelectric field. As further evidence of the phonon-electron coupling, there are reports of acoustic amplification⁽¹²⁾ in piezoelectric semiconductors where the inverse of the above described effect occurs.

Any reporting of, consideration of, or observation of the 3-non interaction to date is unknown to the investigators. Brief notes on the terminology and elementary descriptions of devices commonly referred to in the field of solid state physics is included as an appendix.

Because of the extreme diversity in interpretation of the processes involved, the number of unknowns, and the complexity of a formal analysis, no estimates of the magnitudes of results have been made, but even relatively small indications of the proposed coupling in any of the materials listed previously would be significant. In fact, evidence of such an effect would not only promote further development in the use of the solar cell, but it would also extend its utility as a control device and possibly as a mixed mode amplifier. This investigation is considered to be original only in the sense that such a task has not been openly reported.

The material requirements for conducting the study was met by donations of several silicon solar cells from both Texas Instruments, Inc. and Heliotek, a division of Textron Electronics, Inc. These samples were commercially produced cells and required some preparation for adaption to the laboratory test arrangement. The one desirable feature of such a test sample was that all optimum

fabrication techniques had been incorporated. The major disadvantage, from a documentary test standpoint, was their limited thickness, which curtails the acoustic wavelength range and pulse width for distinguishable reflections of the sound wave. This problem may be alleviated somewhat by use of the sampling oscilloscope as a readout. This does not imply, however, any less complexity of the processes operating within the test sample and as a result, the duration of satisfactory observation of the output is quite small generally compared to the decay of disturbance in the sample.

TEST EQUIPMENT

The pulse generator was capable of delivering single impulse signals of high-voltage for driving for solenoid impactor in addition to providing continuous square-wave signals of up to one megacycle for driving the piezoelectric sound input crystal, which was also utilized for indication of impactor input during single impulse tests. Settings on this unit were non-calibrated and it was thus necessary to provide for calibrated indication of the output on the oscilloscope, using a dual channel preamp.

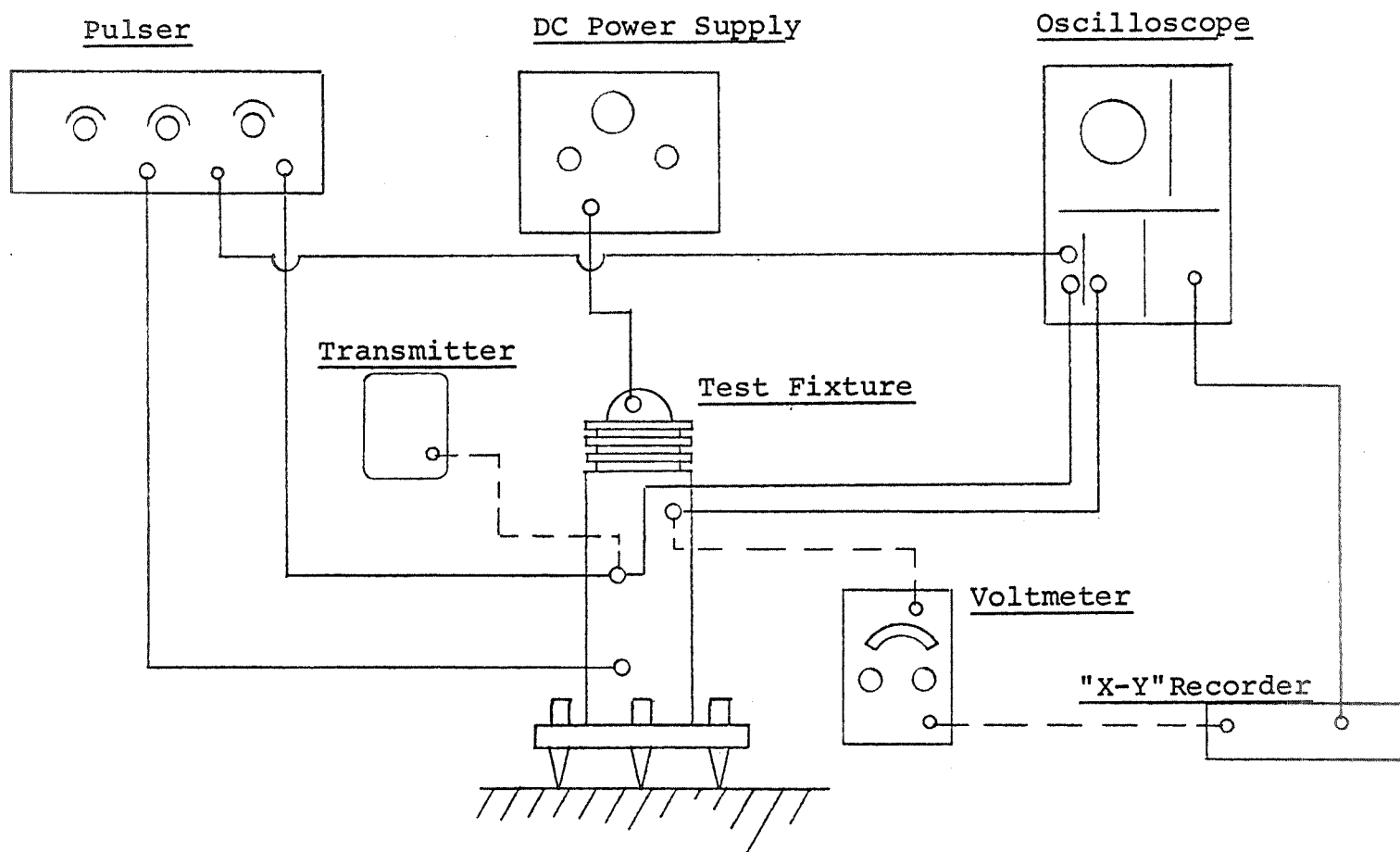
The DC Power Supply was used as the power source for the light in the test fixture. This unit was operated at 12 volts with less than one tenth of one percent ripple.

Both dual channel and sampling type preamps were utilized with the oscilloscope readout. The 50MC range of this basic unit was extended into the gigacycle range with use of the sampling preamp. Maximum sensitivity of the readout was 0.0005mv/cm which thus allowed detection of signals as small as fifty microvolts but without that definition of the stronger signals.

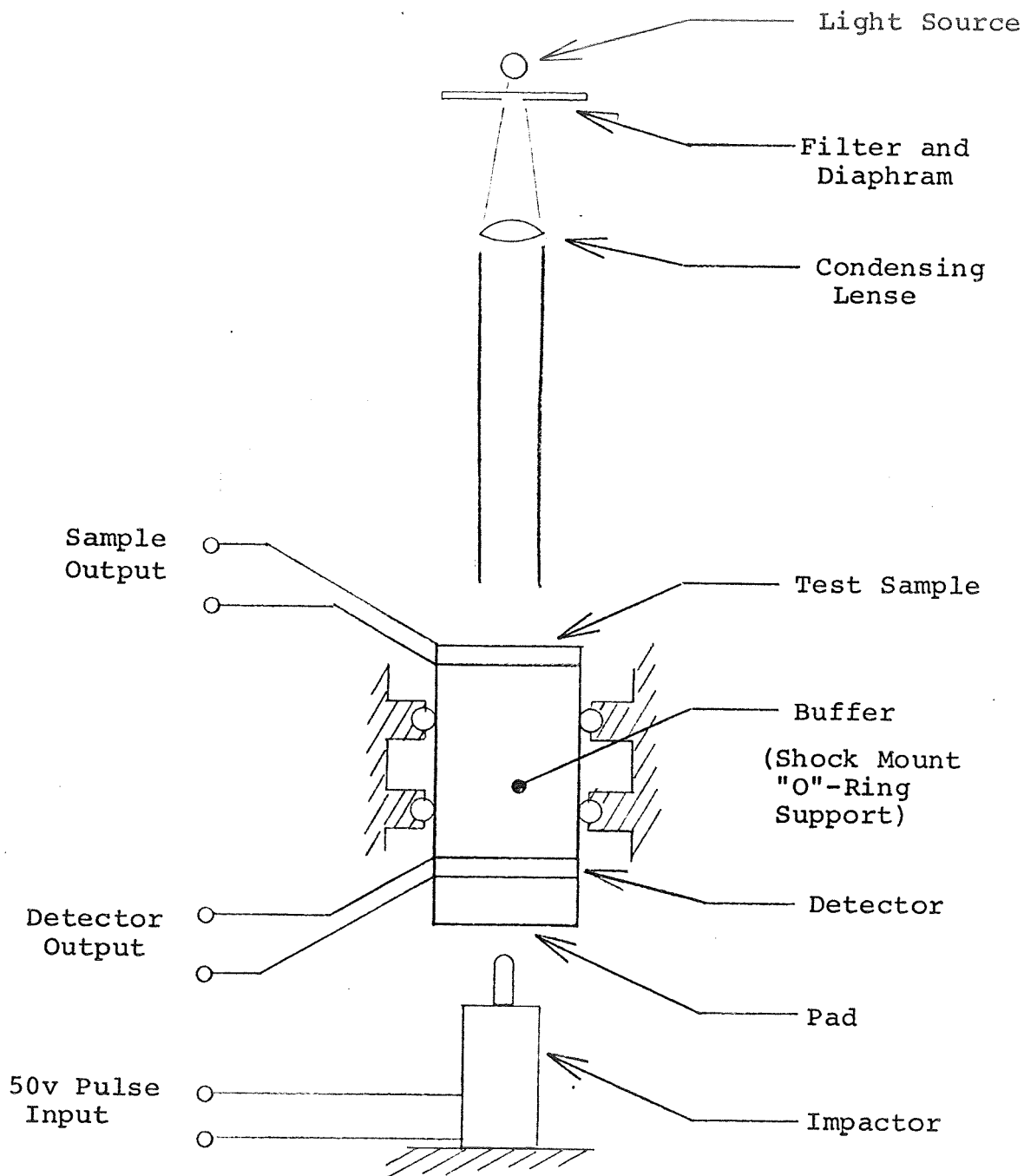
The "X-Y" Recorder was used on two occasions: (1) when employing the sampling preamp with the oscilloscope, and (2) when using the AC Voltmeter as the output detector.

Electrical isolation was a primary consideration in the construction of the test fixture in addition to light sealing. BNC type connections were provided for all electrical lines which were shielded cable. Internally, the test fixture had 100% shielding within the cavities with particularly heavy shielding between the input and output sections. Provision was also made for leveling the fixture on a 3-point suspension. Light filters were insertable above a variable opening diaphragm in the upper portion of the condenser unit.

For higher frequency ranges, between ten and fifty megacycles, a surplus radio transmitter was employed for driving the sound input crystal with some difficulty in operation and regulation. This was partially due to the fact that load matching was not provided for in the test set-up.



ARRANGMENT OF TEST EQUIPMENT



Note: Detector crystal was utilized as continuous frequency sound input with impactor inactive.

TEST DEVICE ARRANGEMENT

LABORATORY PROCEDURE

Test samples were prepared for mounting first by lapping the underside to a flat finish but not polished since this was impractical with the various materials and tools at hand. Some samples were prefabricated and mounted in casings which could not be modified to any extent without destruction of the sample or electrical connections.

With all surfaces cleaned by caustic solution and hydrocarbon solvents, the sample was then mounted on the buffer crystal by one of three means:

- (1) Application of silicone oil
- (2) Indium vapor deposit with pressured assembly
- (3) Silver epoxy joint

Electrical contacts were always made secure by soldered joints, being careful not to impair the mounting by overheating of the sample.

The same method was used in mounting the piezoelectric driver crystals on the opposite surface of the buffer crystal. This crystal was fabricated of quartz with its neutral axis coinciding with the axis of the cylindrical configuration.

Mounted below the driving crystal was the impact cap for protection of the crystal. Various materials were tried for the better transmission of impact without damage to the crystal. Bronze of a relative hard alloy was selected as most desirable.

Arrangement was also provided for spring loading the driver crystal when not using the solenoid impactor. The degree of loading was not increased beyond the point where improvement in transmission ceased.

During the later period of testing, it was found to be more convenient to mount the driving crystal to the buffer by means of pressing the two together with a fluid layer of Salol (Phenyl Salicylate) between, and then allowing the assembly to cool to room temperature. In this way, a range of crystals could

be utilized for better transmission within certain frequency limits.

With use of the dual channel preamp in the oscilloscope the input signal and the output signal could both be observed and compared. Triggering of the oscilloscope was best accomplished by utilizing the delayed output signal that was provided by the pulser.....both for single impulse and continuous low-output-signal tests.

Records of the test sample output were made by photographing the oscilloscope screen using a polaroid camera and mount designed for this purpose. On other occasions, when using the sampling preamp or the voltmeter for output detection, the "X-Y" plotter provided a record of the sample output.

Test variables provided by the test equipment included the following:

- (1) Pulse duration, pulse width, pulse advance, pulse delay, and pulse magnitude
- (2) Light intensity, light spectrum, and light modulation
- (3) Continuous trace detection, single impulse detection, sampling of HF detection
- (4) Frequency of sound input, wave shape of input, frequency, and noise abatement in output.

TEST PROCEDURE

Initial testing of every sample began with frequency scanning with adjustment of pulse width accordingly to that for continuous semetrical wave or periodic pulse with extended neutral period.

Repeating the above then with light sensitive modes. Within each responsive range, the intensity and spectrum was varied to detect any particularly responsive limits.

The test sample output was then recorded with standard light intensity and with varying output loading. Load variation was accomplished by placing a variable resistive load in parallel with the oscilloscope input.

Additional amplification was obtained in certain tests by placing a transformer in the output line between the test sample and the oscilloscope. Also, considerable reduction in interference and noise from stray pick-up was accomplished by placing capacitive loads in parallel with the sample, and in some cases, in series with the sample output.

LABORATORY TEST RESULTS SUMMARY

TYPE	MANF.	DESCRIPTION	RESULTS
Photovoltaic	Vactec RILA 1.13" dia.	Steel-Selenium construction; molecular layers of CdS & CdO. Most sensitive to shorter wavelengths 220ua, rated output.	Responsive to sound: illuminated, lesser response; non-illuminated, higher response. Less than GaAs. No Dark Instability
Photovoltaic	TI	GaAs: Zinc doped, P-type, #1	High output voltage; highly responsive to sound.
Photovoltaic	TI	GaAs: Zinc doped, P-type, #2	Low output voltage; response to sound is barely detectable
Photoresistive	TI	GaAs: Zinc doped, P-type, #3	Highly resistive sample, no voltage output; no response to sound
Photoresistive	RCA #4403	CdS Photocell: 3K ohms @2FC One inch diameter	Dark sample responds vigorously; Lighted sample: no response. Some electrical instability noted.
Photoresistive	RCA SQ-2544	Cadmium-Sulfo-Selenide Photocell 2.4K ohms @2FC; 1/3" Dia.	No dark instability. Sample is responsive to sound W/no illumination.
Photoconductive	Vactec VT-121	CdS @/ spectral pk @ 5150A; 3K @ 2FC; 300K 5 sec. after 2FC	High degree of instability in dark. Responsive to sound when not illuminated.
Photovoltaic	Heliotek	Silicon Solar Cell 2x3cm w/GRID	High Voltage output. No response To sound, with or without illumination

RESULTS AND CONCLUSIONS

Tests were conducted on Gallium Arsenide samples which varied in resistivity due to doping. The most resistive sample (in the range of 50 megohms) showed no response due to sound output. Variation in the sample resistivity when subjected to sound was not investigated. The sample with medium resistivity (approximately 300K) also did not show any response and a minimum voltage output was indicated when subjected to the maximum light intensity....10mv output. The most efficient cell tested showed approximately 100 mv output under normal light intensity. The response to sound was relatively high but was not dependent upon the sample's exposure to light. No shift was observed in the net DC output of the sample. This was to be expected since there was no provision for sound absorption on the far side of the sample. The wave shape was sinusoidal, irregardless of the input shape. The sample did respond to sound as much as 10% of the DC output, but no interaction was observed with the light. The sample output due to sound was highly affected by the degree of loading across the sample output leads. At 300K load (resistive) the sample output was reduced to about 5% as compared to that with 10% with a 10 megohm load. With 500 load, the output was barely detectable.

Silicon solar cells were found to be totally unresponsive to sound input, with or without light exposure.

Several photoresistive devices were tested but there was no indication of direct interaction of light, sound, and electron. A notable effect of sound upon the stability of the electron was observed however in the freshly quenched state of certain samples.

Stability of the inherent electrical dispersion near the P-N junction of photovoltaic devices in some instances is effected by a sound wave traversing the region. It appears that GaA which is zinc doped is highly responsive. Although no shift in response to the optical spectrum was detectable in this series of tests, this is a possibility which could not be confirmed with the

equipment at hand. Even though no 3-non effect could be confirmed, such a device lends itself to use as a unique detective device which could be utilized design of electrical control and detective apparatus.

Appendix

- Semiconductor - A semiconductor is an insulator in which in thermal equilibrium some charge carriers are mobile. At absolute zero a pure, perfect crystal of most semiconductors would be an insulator. The characteristic semiconducting properties are usually brought about by thermal agitation, impurities, lattice defects, or lack of stoichiometry. Semiconductors are understood in practice to be electronic conductors with values of the electrical resistivity at room temperature generally in the range 10^{-2} to 10^9 ohm-cm, intermediate between good conductors (10^{-6} ohm-cm) and insulators (10^{14} to 10^{22} ohm-cm). The electrical resistivity of a semiconductor is usually strongly dependent on temperature. The devices based on the properties of semiconductors include transistors, rectifiers, modulators, detectors, thermistors, and photocells.
- Photon - A quantum energy of electromagnetic radiation. The energy of n photons is $\epsilon = nh\nu = nh\omega$. (h is Planck's const.)
- Phonon - A quantum mechanical unit of energy associated with lattice vibrations.
- Piezoelectric - Deformation of a piezoelectric material is directly proportional to the applied electrical field. These substances are all anisotropic: hemihedral crystals with oblique faces.
- Electorstrictive-Deformation of material is proportional to the square of the applied electrical field.
- Zeeman Effect - Splitting of the energy levels of the electron by application of an external magnetic field.
- Stark Effect - Splitting of the energy levels of the electron by application of an external electric field.

REFERENCES

1. J. J. Loferski, "Recent Research on Photovoltaic Energy Converters," Proceedings of IEEE, May, 1963, pp. 667-674.
2. J. J. Loferski, "Possibilities Afforded by Materials other than Silicon in the Fabrication of Photovoltaic Cells," Acta Electronica, 5(1961), pp. 351-361.
3. Stanley W. Angrist, "Direct Energy Conversion," Allyn and Bacon, Inc., Boston, 1965, p. 100.
4. J. J. Loferski, "Possibilities Afforded by Materials other than Silicon in the Fabrication of Photovoltaic Cells," Acta Electronica, 5(1961), pp. 350-363.
5. S. G. Eckstein, "Acoustoelectric Effect," Journal of Applied Physics, Vol. 35, No. 9, September 1964, p. 2702.
6. R. H. Parmenter, Phys. Rev., 89, 990 (1953).
7. J. C. Slater, "Revs. Modern Phys." Vol. 20, No. 3, 1948 (see Especially p 483).
8. W. Shockley and J. Bardeen, "Energy Bands and Mobilities in Monatomic Semiconductors," Phys. Rev., 77, 407 (1950).
9. J. Mertsching, "Vergleich der Ultraschalleffekte in Piezoelektrischen and Einfachen Deformationspotential-Hableitern," Phys. Stat. Sol. 4, 453 (1964) pp. 453-458.
10. Warren P. Mason, "Physical Acoustics," Volume IV, Part A, Academic Press, pp 24-26.
11. Bardeen, J. and Shockley, W. (1950), Phys. Rev. 80, 72.
12. A. R. Hutson, J. H. McFee and D. L. White, "Ultrasonic Amplification in Cds," Phys. Rev. Letters, Vol. 7, No. 6, Sept. 15, 1961, pp. 237-239.
13. G. Weinreich, (1956), Phys. Rev., 104, 321.
14. M. D. Chapin, C. S. Fuller, and G. L. Pearson, "A New Silicon P-N Junction Photocell for Converting Solar Radiation into Electrical Power," J. Appl. Phys., Vol. 25, pp. 676-677, May, 1954.
15. M. B. Prince, "Silicon Solar Energy Converter," J. Appl. Phys., 26, 534-540, 1955.
16. M. Wolf and M. B. Prince, "New Developments in Silicon Photovoltaic Devices and Their Application in Electronics," Congress for Solid State Physics and Its Applications in Electronics and Communications, Brussels, June, 1958; see also J. Brit IRE, 18, 583-595, 1958.
17. J. J. Lofersky, "Theoretical Considerations Governing the Choice of the Optimum Semiconductor for Photovoltaic Solar Energy Conversion," Journal of Applied Physics, Vol. 27, No. 7, July 1956, p. 779.

18. M. Wolf, "Limitations and Possibilities for Improvements of Photovoltaic Solar Energy Converters," Proc. IRE, July (1960), pp. 1246-1263.
19. Richard H. Bube, "Photoconductivity of Solids," John Wiley and Sons, Inc., New York, New York, 1960, (461 p.).
20. William Shockley, "Electron and Holes in Semiconductors," D. Van Nostrand Co., Inc., New York, New York, 1950 (558 p.).

SUPPLEMENTARY REFERENCES

21. I. Ya Kocherou and I. V. Ostrovskii, "Interaction Between Transverse Ultrasonic Waves and Charge Carriers in Piezoelectric Plates," Soviet Physics, Solid State, Vol. 12, No. 6, December 1970.
22. V. I. Vas'kova and I. A. Viktorov, "Investigation of the Amplification of Ultrasonic Surface Waves in A Cadmium Sulfide Crystal," Soviet Physics-Acoustics, Vol. 15, No. 4. April - June, 1970.
23. C. Fischler, "Acoustoelectric Amplification in a Many-Carrier System," Journal of Applied Physics, Vol. 41, No. 4, 15 March, 1970.
24. A. Rose, "The Acoustoelectric Effects and the Energy Losses by Hot Electrons,"
Part I: "Small Signal Acoustoelectric Effects," RCA Review, Vol. 27, P. 98, March, 1966.
Part II: "Rates of Energy Loss By Energetic Electrons," RCA Review, Vol. 27, P. 600, December, 1966.
Part III: "Large Signal Acoustoelectric Effects," RCA Review, Vol. 28, P. 634, December, 1967.
Part IV: "Field and Temperature Dependence of Electronic Transport," RCA Review, Vol. 30, P. 435, September, 1969.
25. V. G. Skobov, "Quantum Theory of Coupled Electromagnetic Acoustic Waves in Metals," Soviet Physics-Solid State, Vol. 6, No. 9, March, 1963.
26. A. A. Grinberg, "Acousto-Magnetoelectric Effect in Semiconductors," Soviet Physics-Solid State, Vol. 6, No. 7, January, 1965.
27. V. L. Gurevich and B. D. Iskhakman, "On the Excitation of Standing Sound Waves in Piezoelectric Crystals," Soviet Physics-Solid State, Vol. 6, March, 1965.
28. A. I. Morozov, I. B. Kobayakov and I. I. Kisil, "Acoustoelectric Interaction in Hexagone Zn S," Soviet Physics-Solid State, Vol. 8, No. 3, September, 1966.